Ion-surface interaction potentials from alkali-ion–metal scattering below 500 eV

D. M. Goodstein, R. L. McEachern, and B. H. Cooper
Laboratory of Atomic and Solid State Physics, Cornell University, Clark Hall, Ithaca, New York 14853-2501
(Received 30 November 1988)

Classical-trajectory calculations using an ion-surface potential which is represented as a sum of ion-atom pair potentials plus an attractive imagelike potential are compared to experimental results for the scattering of Na^+ and K^+ from Cu(110) in the energy range 100 eV $\leq E_0 \leq$ 400 eV. The strong focusing of ion trajectories on this surface greatly enhances the sensitivity of the scattering to the form of the ion-surface interaction potential. We achieve very good agreement between calculated and experimental spectra using pair potentials computed within the Hartree-Fock approximation.

INTRODUCTION

The ability to directly probe ion-surface interactions in the hyperthermal energy range ($\approx$10 to 500 eV) via scattering experiments is a relatively recent development. It is therefore not surprising that a clearer understanding of the ion-surface interaction in this energy range is still being sought. The natural starting point has been to try to extend to hyperthermal energies the interaction models that have been successful at higher energies. For example, low-energy ion scattering (LEIS), which uses ion beams with energies from approximately 500 eV to 10 keV for surface structure and composition analysis, involves ion-surface interactions that are fairly well understood. A number of experimental studies have shown that approximating the ion-surface interaction by a sum of ion-atom pair potentials, based on either the semiclassical Thomas-Fermi method[1] or the Gordon-Kim method of overlapping charge densities,[2] can reproduce both the energy and angular distributions observed in alkali and noble gas LEIS from metal surfaces. Furthermore, since the scattering is dominated by the short-range part ($r_{\text{ion-atom}} \lesssim 1$ Å) of the ion-atom potential, the trajectory of an incident ion may be treated as a series of sequential binary collisions (SBC) involving one surface atom at a time. These simple potentials and scattering models work because the scattering at these energies is not especially sensitive to the longer-ranged ($r_{\text{ion-atom}} > 1$ Å) part of the ion-surface interaction. There is, however, considerable current interest in the behavior of the ion-surface potential at these larger separations. For example, the complicated processes that occur during reactive ion etching and ion beam modification of materials involve ion-surface interactions spanning an energy range from many keV's down to a few eV's. Understanding the ion-surface interaction at very low energies is therefore essential for developing detailed models of these technologically important processes. In addition, the charge-transfer mechanisms which play such a dominant role in surface- or adsorbate-induced catalysis also occur in hyperthermal ion-surface interactions,[3,4] and may therefore be studied by scattering experiments.

Recent work at ion energies below 100 eV has shown that it is necessary to treat both the ion trajectory and the interaction potential that determines it in greater detail than is required at higher energies. The sequential binary collision approximation is no longer tenable at these energies; classical-trajectory calculations which allow the incident ion to interact with several surface atoms simultaneously must be used. Hartree-Fock and related approximations[5] have been shown, in a very limited number of systems, to provide ion-atom pair potentials which reproduce most of the features seen in hyperthermal scattering spectra,[6] which the Thomas-Fermi and Gordon-Kim potentials cannot. The need to include attractive imagelike forces in the calculation of hyperthermal scattering spectra has been demonstrated for K^+-W(110).[7,8] Evidence for a breakdown of the approximation of the repulsive part of the ion-surface potential as a sum of pair potentials has also been reported.[8] Continued work on new systems over a wider energy range is necessary to examine the generality of the current picture of hyperthermal ion-surface interactions, which to date rests on experiments involving very few ion-target combinations. In this paper we present experimental and theoretical work on the scattering of 100- to 400-eV Na^+ and K^+ from Cu(110), which provides insights into the hyperthermal ion-surface interaction.

In general, an ion-surface collision involves two major classes of interactions which, depending on the ion energy and ion-surface combination, may be considered more or less separately. The first class involves the adiabatic rearrangement of the electronic degrees of freedom of the incident ion and the surface. At small ($r < 2.0$ Å) ion-atom separations, the large overlap of the ion and surface-atom electronic distributions leads to a strongly repulsive ion-surface potential-energy curve, while at large ion-surface separations, the attraction of the ion to its induced image charge will accelerate it toward the surface. This "electronically elastic" part of the ion-surface interaction may be represented by a conservative potential-energy function that depends solely on the posi-

 ©1989 The American Physical Society

tions of the ion and surface atoms. The forces induced by this conservative potential are responsible for the deflection of the incident ion and the transfer of some of the ion's momentum and kinetic energy to the surface. The second class of ion-surface interactions consists of electronically inelastic processes, which include both neutralization[4] and excitation of the scattered ion, as well as electronic "friction" effects.[9] Finally, it must be borne in mind that the energy that is deposited at the surface by the ion, initially in the form of recoil energy imparted to individual surface atoms, may be dissipated in a number of ways, for example through the creation of electronic excitations, vacancies, and phonons.[10] Since we are concerned only with the fate of the primary ion, we will not consider these modes of energy dissipation further, but they can be extremely important in sputtering and other surface-modifying processes.

To date, most attempts to determine the repulsive part of the ion-surface interaction by scattering experiments have used alkali ion beams and metal surfaces. On *clean* metal surfaces, the low ionization potential of the alkalis guarantees a large scattered ion fraction; in addition, the neutralization probability is generally only weakly dependent on the scattered ion trajectory[4,11] for these systems, and thus the sole effect of neutralization is a uniform reduction in the scattered ion intensity. We can therefore compare relative peak intensities arising from different scattering trajectories without having to correct for differences in neutralization probability (although any analysis involving *absolute* scattering cross sections still requires either neutral particle detection or a quantitative model of the neutralization probability).

The great sensitivity of hyperthermal alkali ion scattering to the ion-surface interaction potential is intimately related to the role of multiple collisions in the scattering process, and how their role changes with incident ion energy. In the absence of multiple collisions, an incident ion scatters from a single surface atom (a single scattering event), and the ion energy spectrum consists of one peak whose energy is determined solely by the ion-to-surface-atom mass ratio and the total scattering angle. This can be observed in higher-energy scattering ($E_0 > 10$ keV) with noble gas ions, which, due to their very high neutralization probability, rarely survive multiple collisions. The energy spectra of scattered alkali ions, even at very high incident energies, usually exhibit an additional peak at a higher energy than the single scattering peak. This peak may be attributed to two consecutive, approximately equal-angle collisions with two adjacent surface atoms along an atomic chain (a double scattering event). The energy of this double scattering peak is likewise determined almost entirely by the mass ratio and the total scattering angle. The intensity ratio of the single to double scattering peaks, however, depends on both the atomic spacing[12] along the chain and the ion-atom scattering potential.[13] At lower incident ion energies ($E_0 \lesssim 4$ keV), other types of multiple collisions can occur. Nearby atoms which are not involved in the main collision can significantly perturb the incoming and outgoing ion trajectory. Their contribution is of course strongly dependent on their positions relative to the main collision site, and on the range of the ion-atom potential. These atoms can be located either along the chain containing the main collision partner(s) (leading to quasisingle and quasidouble scattering[13]), or on adjacent chains (leading to zig-zag and focused scattering). As the incident energy is lowered still further ($E_0 < 500$ eV), multiple scattering effects can dominate the ion spectra. As will be shown in this paper, this can lead to a dramatic dependence of the positions and relative intensities of peaks in the energy spectra on both the incident energy and surface geometry.

Previous studies of hyperthermal ion-surface interactions have examined the scattering of potassium[7,8] from W(110) at energies below 50 eV, and the scattering of potassium and sodium from Ag(111) at energies from 10 to 100 eV.[6] In those experiments, the majority of scattered ions did not penetrate the first layer. In the present work, however, we find that most of the scattering comes from the second layer. This is due both to the higher-energy beams used (100 to 400 eV), and the very open structure of the (110) face of copper (Fig. 1), which leads to the phenomenon of focusing. Focusing occurs when the forces from adjacent chains of first-layer atoms steer incident ions towards second-layer atoms. The (110) face of face-centered-cubic crystals is ideal for focused scattering, since the $\langle 001 \rangle$ direction consists of closely spaced chains of first-layer atoms, with second-layer atoms in between. As can been seen in Fig. 1, an ion which scatters from the second layer in the $\langle 001 \rangle$ direction interacts with first-layer atoms at distances greater than 1.2 Å. In the $\langle 1\bar{1}0 \rangle$ direction, this distance increases to 1.8 Å. Depending on the interaction potential and incident ion energy, scattering from the second layer can be quite sensitive to the influence of first-layer atoms at these separations.

We have found that the energy distributions of Na^+ and K^+ scattered from Cu(110) in the energy range 100 eV $< E_0 <$ 400 eV are strongly affected by the presence of first-layer atoms, even though the bulk of the scattering originates from second-layer atoms. This sensitivity makes the energy distributions useful for testing models for the ion-surface interaction potential. We have achieved quite good agreement between calculated and measured energy spectra by assuming an ion-surface potential which is a sum of individual alkali ion-copper atom pair potentials and an attractive imagelike potential. The pair potentials are computed within the Hartree-Fock approximation and contain no adjustable parameters. In the work presented here, we have examined the changes in energy spectra for 90° specular scattering as a function of incident ion energy and azimuth, and the sensitivity of these changes to the interaction potential. An analysis of the full energy and angular distributions of Na^+ scattered from Cu(110) will be given elsewhere.[14]

The rest of the paper is organized as follows. The experimental technique used to measure ion scattering spectra is reviewed briefly in Sec. I. The main experimental results and their interpretation in terms of specific scattering mechanisms are presented in Sec. II. Section III outlines the classical-trajectory calculations used to

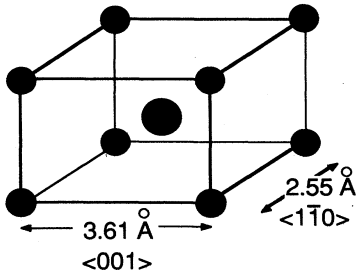

FIG. 1. The first three layers of the Cu(110) surface. The ⟨001⟩ atomic rows are 2.55 Å apart, while the ⟨1$\bar{1}$0⟩ rows are separated by 3.61 Å. The first-to-second-layer distance is approximately 1.18 Å, due to relaxation of the surface.

obtain simulated energy spectra for comparison with experiment, and the Hartree-Fock energy calculations are described. In Sec. IV, calculated spectra are compared to experiment, and the quality of agreement is discussed. Conclusions are presented in the final section.

I. EXPERIMENTAL TECHNIQUE

The experiments were performed in an UHV ion scattering system which has been described in detail elsewhere.[15] Alkali ions are produced by thermal emission from a hot ($\approx$1100 °C) alkali-embedded tungsten source. During transport of the beam from the source to the scattering chamber, the ions are mass selected using a Wien filter, and neutral rejection is accomplished with a 90° spherical-sector electrostatic analyzer. The beam on target had currents of several nanoamperes in a 3-mm-diameter spot, and an energy spread characteristic of the thermal source (less than 0.5 eV). The half-angle divergence of the beam was less than 2°. Scattered ions are detected with a 180° electrostatic analyzer which has a 1° half-angle acceptance and 1% energy resolution, and which is mounted on a rotating table. The Cu(110) sample was mounted on a three-axis manipulator which, in combination with the detector rotation, allows access to all scattering geometries not excluded by the finite size of the detector and final beam lenses (total scattering angles $\lesssim$127°). The total scattering angle and incident beam angle relative to the crystal normal can be set to an accuracy of 0.1°. Low-energy electron diffraction (LEED) and ion scattering were used to align the scattering plane with the ⟨1$\bar{1}$0⟩ or ⟨001⟩ azimuths to within ±0.5°.

The Cu(110) crystal was initially cleaned by cycles of sputtering with 500-eV Ar^+ and annealing at 650 °C. This was repeated until a 30-min anneal at 550 °C brought no contaminants to the surface as determined by Auger electron spectroscopy. The standard cleaning procedure during experiments consisted of sputtering for 30 s with a 1.5-μA beam of 500-eV Ar^+ followed by a 30-min anneal at 550 °C. In these experiments, it was possible to take many energy spectra between surface cleanings. Typical beam doses per spectrum were 2×10^{13} ions/cm^2 for 100-eV beams. Even after 20 spectra, this corresponds to a total dose of less than 0.5 ions per surface unit cell. Long exposures to the alkali beam resulted in a uniform reduction in the scattered ion intensity, with no change in the relative peak heights or peak positions. The variation of the scattered ion intensity as a function of alkali coverage has been examined in detail elsewhere,[4] and may be attributed to an increase in the resonant charge-transfer probability for increasing coverage. No changes in the energy spectra were seen that could be attributed to sputter damage by the incident ion beam.

II. EXPERIMENTAL RESULTS

Figures 2–4 show measured energy spectra (uncorrected for the $1/E$ variation of the detector's energy acceptance as a function of ion energy E) for 90° specular scattering of Na^+ and K^+ from Cu(110) for incident energies E_0 of approximately 100, 200, and 400 eV. Using classical-trajectory calculations[16] it is possible to relate peaks in the measured energy spectra to specific types of scattering trajectories.[17] The Na^+ spectra along the ⟨001⟩ azimuth (Fig. 2) all exhibit a large peak, well

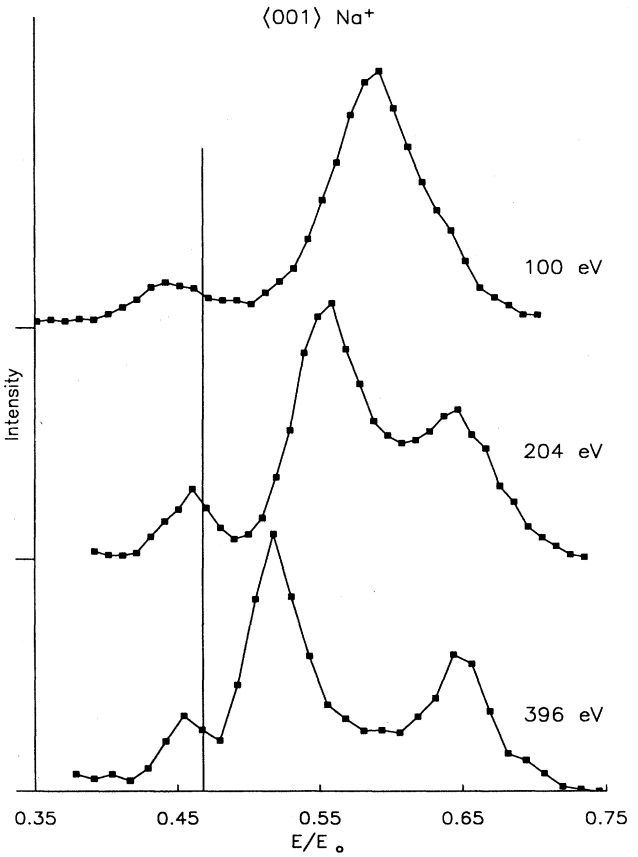

FIG. 2. Experimental spectra showing intensity (arbitrary units) vs reduced energy (E_{final}/E_0) for the 90° specular scattering of Na^+ along the ⟨001⟩ azimuth of Cu(110) at incident energies of 100, 204, and 396 eV. The vertical line at $E/E_0=0.47$ is the reduced energy value, as determined by energy and momentum conservation, for a pure single scattering of sodium by copper through an angle of 90°.

above the kinematic energy for binary single scattering (vertical line at $E/E_0=0.47$), which is due to focused single (FS) scattering from second-layer atoms. The lowest energy peak visible in the three spectra in Fig. 2 is a mixture of single scattering from first-layer copper atoms and some zig-zag scattering. The highest energy peak visible in the 200- and 400-eV spectra is due to double scattering events, in which the incident sodium ion undergoes approximately equal-angle collisions with two adjacent copper atoms along a chain.

The presence of a large focused single scattering peak in these spectra can be understood in terms of the special arrangement of atoms near the Cu(110) surface (Fig. 1). The chains of first-layer atoms produce restoring forces which are perpendicular to the scattering plane [the $(1\bar{1}0)$ plane for $\langle 001 \rangle$ scattering], and which vanish over the second-layer chains. In the absence of these restoring forces, only those ions with impact parameters precisely over a chain would remain in the scattering plane (excluding zig-zag scattering). This is the case for scattering along a first-layer chain of atoms. However, for second-layer scattering, these restoring forces guarantee that ions with impact parameters well off the second-layer chain are focused towards it. Therefore, a larger range of impact parameters contribute to the measured spectrum from regions where focusing is occurring than from unfocused regions. It is precisely these out-of-plane forces that ensure a large intensity for the FS peak relative to the first-layer single scattering peak (lowest energy peaks in Fig. 2), which is unfocused.

The first-layer atoms also produce forces parallel to the scattering plane. These forces allow the first-layer atoms to contribute to the total in-plane deflection of the scattered ion. It is easily shown by energy and momentum conservation[17] that less kinetic energy is lost by the ion to the surface when more atoms are involved in deflecting the ion through a given in-plane scattering angle. Therefore, these in-plane forces will shift the FS scattering peak to a higher final energy than the first-layer single scattering peak. The shift is so large at 100 eV that the FS peak is degenerate with the double scattering peak (see Fig. 2). As the incident energy is increased from 100 to 400 eV, the in-plane forces from the first-layer atoms become less effective in deflecting the incident sodium

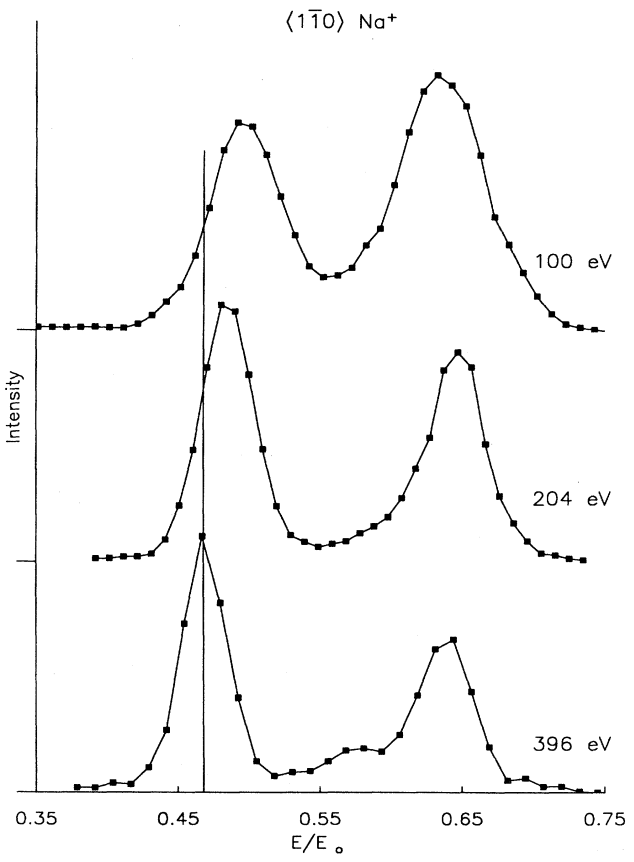

FIG. 3. Experimental spectra showing intensity (arbitrary units) vs reduced energy for the 90° specular scattering of Na^+ along the $\langle 1\bar{1}0 \rangle$ azimuth of Cu(110) at incident energies of 100, 204, and 396 eV. Vertical line is the same as in Fig. 2.

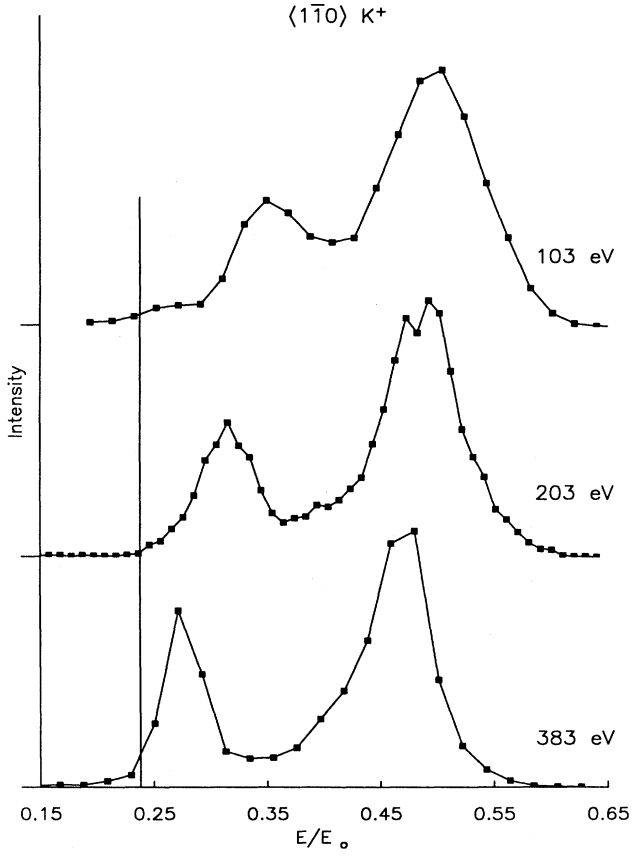

FIG. 4. Experimental spectra showing intensity (arbitrary units) vs reduced energy for the 90° specular scattering of K^+ along the $\langle 1\bar{1}0 \rangle$ azimuth of Cu(110) at incident energies of 103, 203, and 383 eV. The vertical line at $E/E_0=0.24$ is the reduced energy value for a pure single scattering of potassium by copper through an angle of 90°.

ion, and the focused single scattering peak energy approaches that of the first-layer single scattering peak, as expected.

The spectra for 90° specular Na^+ scattering along $\langle 1\bar{1}0 \rangle$ show less dramatic variation with incident energy (Fig. 3). The low-energy peak does not shift appreciably in energy as the incident energy varies from 100 to 400 eV. Trajectory analysis indicates, however, that focused scattering from the second layer still provides the dominant contribution to the spectra. If we recall that the intensity enhancement of the FS peak relative to the first-layer single scattering peak is due to out-of-plane forces from the first layer, while the energy shift of the FS peak is governed by the in-plane forces, the dominance of focused scattering even in the absence of appreciable energy shifts is understandable. First-layer $\langle 1\bar{1}0 \rangle$ chains of atoms are separated by a distance $d_{1\bar{1}0}=3.61$ Å, which is 30% greater than the distance between $\langle 001 \rangle$ chains ($d_{001}=2.553$ Å). Consider an incident ion passing a first-layer atom such that, at closest approach, it is a height Δz above the surface and x to one side of the atom. The ion-atom separation is therefore $[x^2+(\Delta z)^2]^{1/2}$. The in-plane force from this first-layer atom is proportional to $\Delta z/[x^2+(\Delta z)^2]^{1/2}$, while the out-of-plane force is proportional to $x/[x^2+(\Delta z)^2]^{1/2}$. The in-plane component is therefore $\Delta z/x$ times the out-of-plane component. If we keep the ion position fixed, and increase d (which increases x), the in-plane force will decrease faster than the out-of-plane force. This is why we still see the intensity enhancement characteristic of focused scattering in the $\langle 1\bar{1}0 \rangle$ spectra, even when the energy shift is no longer appreciable.

We can partially compensate for the increase in d in going from the $\langle 001 \rangle$ to $\langle 1\bar{1}0 \rangle$ azimuth by scattering an ion that has a longer-ranged interaction with the surface. The 90° specular K^+ scattering along $\langle 1\bar{1}0 \rangle$ (Fig. 4) demonstrates the great sensitivity of the focusing to the range of the ion-surface interaction potential. Unlike the $\langle 1\bar{1}0 \rangle$ Na^+ scattering, the $\langle 1\bar{1}0 \rangle$ K^+ spectra show a very large energy shift for the FS peak. This is because the K^+-Cu interaction potential is large enough for first-layer atoms to produce appreciable in-plane forces over the second-layer chains even in this azimuth. As in the $\langle 001 \rangle$ sodium spectra, the first-layer single scattering peak is visible below the FS peak in the 100-eV $\langle 1\bar{1}0 \rangle$ K^+ spectrum, which is not true of the 100-eV $\langle 1\bar{1}0 \rangle$ Na^+ spectrum (Fig. 3). Note that this top-layer peak appears above the kinematic scattering energy for a single collision, even though it is unfocused. This shift is due to forces from atoms in the *same* first-layer chain as the main collision site (a quasisingle scattering event). When the potassium incident energy has increased to 200 eV, the first-layer single peak is obscured by the FS peak, which has moved down in energy.

III. TRAJECTORY AND POTENTIAL CALCULATIONS

As stated in the introduction, we do not expect the sequential binary collision approximation to provide an adequate description of the ion trajectories in this energy regime, especially in the presence of strong focusing. We have therefore performed our ion scattering simulations with the program SAFARI,[16] which numerically integrates the classical equations of motion for the incident ion interacting with several surface atoms simultaneously. Although forces between surface atoms are ignored, the surface atoms are bound harmonically to their equilibrium lattice sites by isotropic springs with spring constants determined by the bulk vibrational amplitude of copper ($\simeq 0.07$ Å). At the beginning of each trajectory, a set of initial displacements and velocities is randomly assigned to the surface atoms from a Gaussian distribution appropriate to the surface temperature and spring constants.[18] Impact parameters were chosen randomly within the surface unit cell. A complete spectrum (which requires the calculation of $\simeq 90\,000$ trajectories) represents an average over impact parameters and thermal displacements and velocities. The thermal averaging contributes to the widths of the energy peaks, and can change their relative intensities, but does not appreciably alter their positions. The spring forces themselves do not directly affect the scattering dynamics, since the collision times are much shorter than typical vibration times. The Cu(110) surface used in the simulations consisted of three layers, with the first- to second-layer spacing contracted by 7.5% and the second- to third-layer spacing expanded by 2.5% with respect to the bulk copper spacing, as determined by Copel *et al.*[19] using medium energy ion scattering. Our results were insensitive to the second- to third-layer spacing, as well as to variations of the first- to second-layer spacing within the experimental uncertainty of Copel *et al.* ($\pm 1.5\%$).

Since the incident ion energies used here are much greater than typical chemisorption energies, the scattering experiments probe predominately the repulsive part of the ion-surface potential. It has been demonstrated that the scattering of higher-energy ($E_0 \geq 500$ eV) ions from surfaces can be accurately modeled by assuming a repulsive interaction potential which is a sum of individual spherically symmetric ion-surface atom pair potentials. This model has also been used at much lower energies,[7,8] and we will assume that the major features of the repulsive part of the ion-surface interaction can be represented in this way for the energies of interest here. The ion-atom pair potentials used in these simulations were calculated within the Hartree-Fock approximation using the program GAUSSIAN86.[20] For each alkali ion A^+ and ion-copper atom separation r, the scattering potential $V(r)$ was taken as the total-energy difference $E(A^+$-Cu;$r)-E(A^+)-E$(Cu) between the ion-atom molecule and the isolated ground-state alkali ion and copper atom. The copper atom was represented by an uncontracted $(13s,7p,5d)$ (Ref. 21) Gaussian basis with additional p polarization functions.[22] The Na^+ and K^+ bases were $(10s,4p)$ and $(14s,9p)$,[23] respectively. The scattering potentials (Fig. 5) were calculated at 17 separations between 0.5 and 2.0 Å and fit to a sum of two repulsive exponentials.

For the range of separations considered above, only the repulsive part of the Hartree-Fock potential is sampled. At greater separations, the alkali ion polarizes the copper atom electron distribution, which leads to a weakly at-

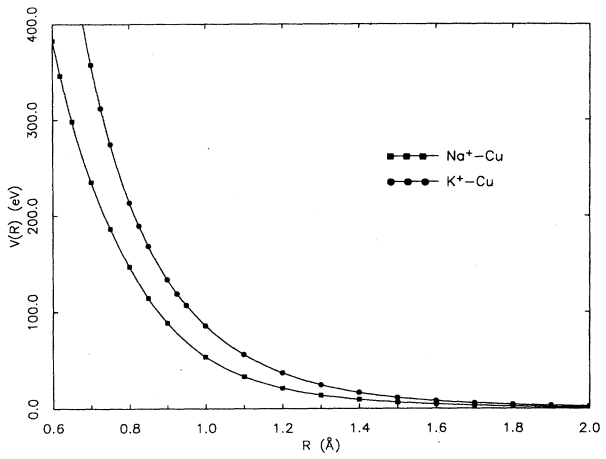

FIG. 5. Potential energy $V(R)$ vs interatomic separation R for Na^+-Cu and K^+-Cu diatomics, calculated within the Hartree-Fock approximation. Lines are drawn to guide the eye.

tractive potential. At a real metallic surface, however, the attractive part of the ion-surface potential is due to the response of the delocalized conduction electrons, and cannot be reproduced by a sum of attractive polarization potentials from ion-atom pairs. It is necessary to include this attraction at some level, however, since for large ion-surface separations the ion will induce an image charge in the metal that can affect its trajectory. The attractive part of the ion-surface interaction is included by adding a potential to the trajectory calculations that depends solely on the perpendicular ion-surface separation, and which goes over to the classical image potential at large separations. It is of the form

$$V(z)=\begin{cases}\dfrac{-e^2}{\left[16z^2+\dfrac{e^4}{V_{\min}^2}\right]^{1/2}} & \text{for } z>0 \quad (1a)\\ -V_{\min} \quad \text{for } z<0\ , & (1b)\end{cases}$$

where $z=0$ corresponds to the plane containing the top-layer atoms. For reasonable values of $V_{\min}$ (small compared to the incident energy), the main effect of this attractive potential is to induce small changes in the positions of the energy peaks in the calculated spectra. It has very little effect on relative peak intensities. This form has been used previously at lower incident energies ($E_0<50$ eV) with systems where scattered ions rarely penetrated the first layer.[7,8] The behavior of this attractive potential for $z\leq 0$ was not directly probed by such experiments. In the present work, however, the majority of scattering is from second-layer atoms, and so the attractive potential near and below the surface may be more important. Treating $V_{\min}$ as a free parameter, we have found the best agreement between calculations and experiment with $V_{\min}=3$ eV, for both Na^+ and K^+. We do not, however, expect $V_{\min}$ to be independent of ion species in general.

Inelastic electronic energy losses were not included in the simulations presented here. The ions are moving too slowly for plasmon excitation, and no features attributable to electronic excitations of the scattered particle were seen. This still leaves open the possibility of electron-hole pair creation in the metal. In order to estimate its importance, we performed several simulations using an effective medium model[24] for the energy loss to electron-hole pairs. The electron scattering cross section at the Fermi level, $\sigma(n,Z)$, for an atom of charge Z embedded in a uniform electron gas of density n can be calculated within the effective medium approximation. The electronic energy loss per unit distance dW/dr (Ref. 9) is then given by

$$dW/dr=-nk_F\sigma v_{\text{ion}}\ , \quad (2)$$

where v_{ion} is the ion velocity and k_F is the Fermi wave vector of the metal. For a constant electron density of 0.0125 a.u., which is the valence density of copper, 400-eV K^+ will lose approximately 0.5 eV/Å. The copper electronic density is, however, not constant throughout the ion's trajectory. This was accounted for by taking the electronic density, $n(\mathbf{r}_{\text{ion}})$, at each point along the ion's trajectory to be the sum of contributions from free copper atomic densities, n_0, centered at the crystal lattice sites $\mathbf{R}_i$:

$$n(\mathbf{r}_{\text{ion}})=\sum_i n_0(\mathbf{r}_{\text{ion}}-\mathbf{R}_i)\ . \quad (3)$$

Such a sum of free atomic densities can reproduce the true metal electron density to within roughly 20%. This leads to a position-dependent energy loss:

$$dW/dr=-n(\mathbf{r}_{\text{ion}})k_F(\mathbf{r}_{\text{ion}})\sigma(Z,n(\mathbf{r}_{\text{ion}}))v_{\text{ion}}\ . \quad (4)$$

This gave energy peak shifts of less than 2%, and so was not used further. The Firsov[25] model of inelastic energy losses, which is more appropriate for situations involving isolated binary collisions,[10] was not considered.

IV. COMPARISON OF CALCULATIONS AND EXPERIMENT

For these studies, we are mainly interested in the relative intensities and positions of the peaks appearing in the energy spectra. We have therefore normalized the experimental and calculated spectra so that the focused single scattering peak heights are approximately the same in both. This does not affect the peak positions or relative intensities. To ensure adequate statistics in the simulations, the angular acceptance of the simulated detector was ±3°, as compared to an experimental detector acceptance of ±1°. It was verified that the relative peak heights and peak positions in the simulated spectra did not vary with detector acceptance from ±1° to ±3° (except for the statistical fluctuations associated with having fewer trajectories in the smaller detectors). Since we have not attempted to compare absolute cross sections, no correction for the neutralization of scattered particles was attempted. Similarly, we have not included the initial beam divergence (~±2° at 100 eV) in the simula-

tions. All calculated spectra were folded with the experimental detector's energy transmission function, which for a 180° electrostatic detector varies linearly with detection energy (energy acceptance ΔE is proportional to E).

In Fig. 6, calculated energy spectra for 90° specular scattering of Na^+ along the $\langle 001 \rangle$ azimuth of Cu(110) are compared with experiment. The decrease of the focused single scattering energy as the ion incident energy is increased is very well reproduced. Furthermore, the calculated and experimental peak energies agree to 1% or better for all peaks. The ordering of the peak intensities, with the FS peak largest, the double scattering peak smaller, and the top-layer single peak smallest, is also reproduced in the calculated spectra.

The $\langle 1\bar{1}0 \rangle$ Na^+ calculated spectra are shown in Fig. 7. Here, too, the overall agreement between calculations and experiment is quite good. The calculations exhibit the observed increase in intensity of the FS scattering peak relative to the double peak with increasing incident energy, and the energy peak positions are nicely reproduced.

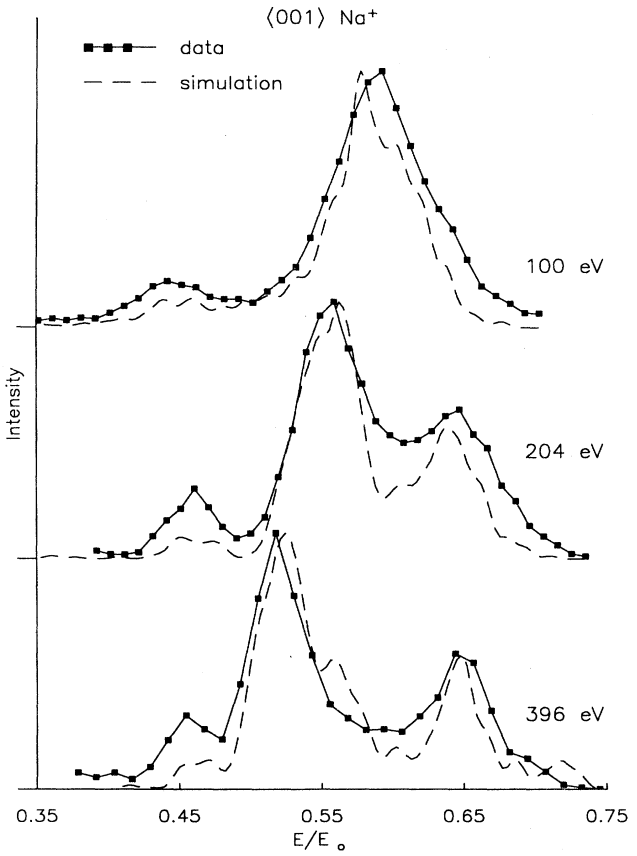

FIG. 6. Comparison of measured and calculated spectra for 90° specular scattering of Na^+ along the $\langle 001 \rangle$ azimuth of Cu(110) at incident energies of 100, 204, and 396 eV. Calculated spectra are corrected for the transmission of the detector. The calculation was performed with the Hartree-Fock Na^+-Cu pair potential and an attractive imagelike potential with $V_{min} = 3$ eV.

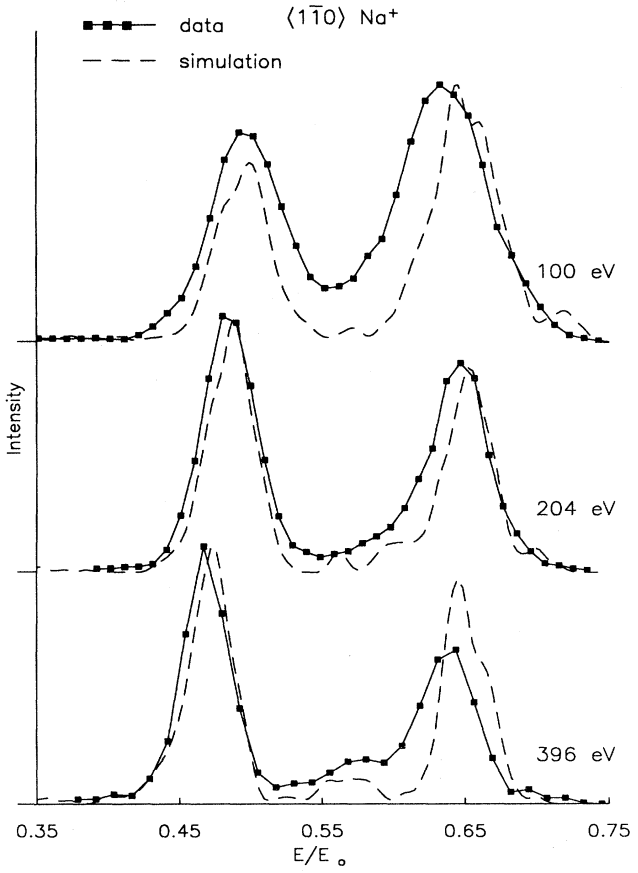

FIG. 7. Comparison of measured and calculated spectra for 90° specular scattering of Na^+ along the $\langle 1\bar{1}0 \rangle$ azimuth of Cu(110) at incident energies of 100, 204, and 396 eV. The calculation was performed with the Hartree-Fock Na^+-Cu pair potential and $V_{min} = 3$ eV.

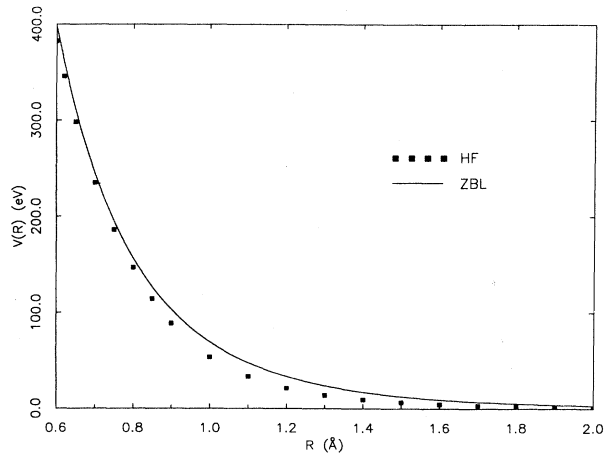

FIG. 8. Comparison of Hartree-Fock (HF) and Ziegler-Biersack-Littmark (ZBL) potentials for Na^+-Cu pairs. The ZBL potential is larger than the HF potential for all energies of interest here, and dies off more slowly with distance.

An obvious discrepancy between the measured and calculated spectra is that in the ⟨001⟩ azimuth, the simulated first-layer single scattering peaks are too small relative to the FS peaks at each of the three incident energies (they are also too small in the 100-eV ⟨1$\bar{1}$0⟩ K^+ spectrum). This may be due to an underestimate of the thermal vibration amplitudes. To a first approximation, the first-layer single scattering energy and intensity are independent of atomic displacements, while the amount of focused scattering, which relies on the precise alignment of several atoms, would be decreased by an enhancement of the vibration amplitudes. A medium-energy ion scattering study of the Cu(110) surface found enhanced vibrational amplitudes near the surface.[19] Our simulations did not show any consistent improvement when we included these enhanced amplitudes; however, an exhaustive study of the effects of different amplitudes, including anisotropic vibrations, has not been performed.

The quality of the agreement between the calculated and experimental spectra we have achieved using Hartree-Fock potentials can be appreciated by comparing with spectra calculated with other candidate potentials. An obvious choice is the Ziegler-Biersack-Littmark (ZBL) potential (Fig. 8),[26] which is based on a Gordon-Kim approximation[2] to the interaction energy of two overlapping atoms, and which has been successfully used to describe the scattering of Li^+, Na^+, and K^+ from Mo(001) in the energy range 500–2500 eV.[27] In Fig. 9 we compare calculated ZBL spectra with experiment for 90° specular Na^+ scattering from Cu(110) along the ⟨001⟩ azimuth. The calculated 100-eV spectrum shows very little resemblance to the data. V_{min} was 3 eV in these calculations as well; the agreement between the calculated and measured spectra was not improved by varying V_{min}. At higher incident energies, the ZBL simulations begin to resemble the data. The 200- and 400-eV ZBL spectra both exhibit the top-layer single, FS, and double scattering peaks seen in the data. However, the FS scattering peak appears at far too high an energy in both calculated spectra, and the FS scattering to double scattering intensity ratio is much too small. It is interesting to note that the ZBL potential reproduces the top-layer single scatter-

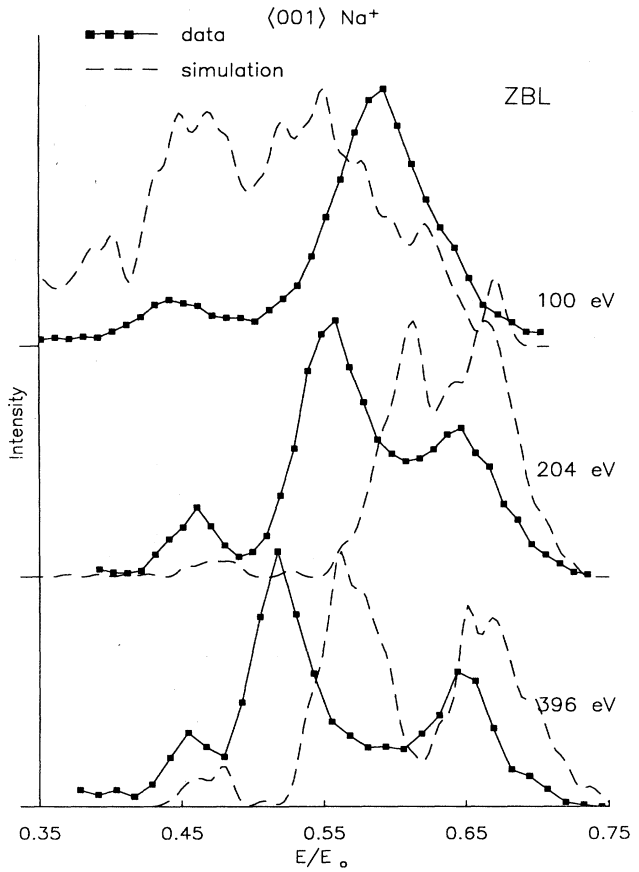

FIG. 9. Comparison of measured and calculated spectra for 90° specular scattering of Na^+ along the ⟨001⟩ azimuth of Cu(110) at incident energies of 100, 204, and 396 eV, using the Ziegler-Biersack-Littmark Na-Cu pair potential and $V_{min}=3$ eV.

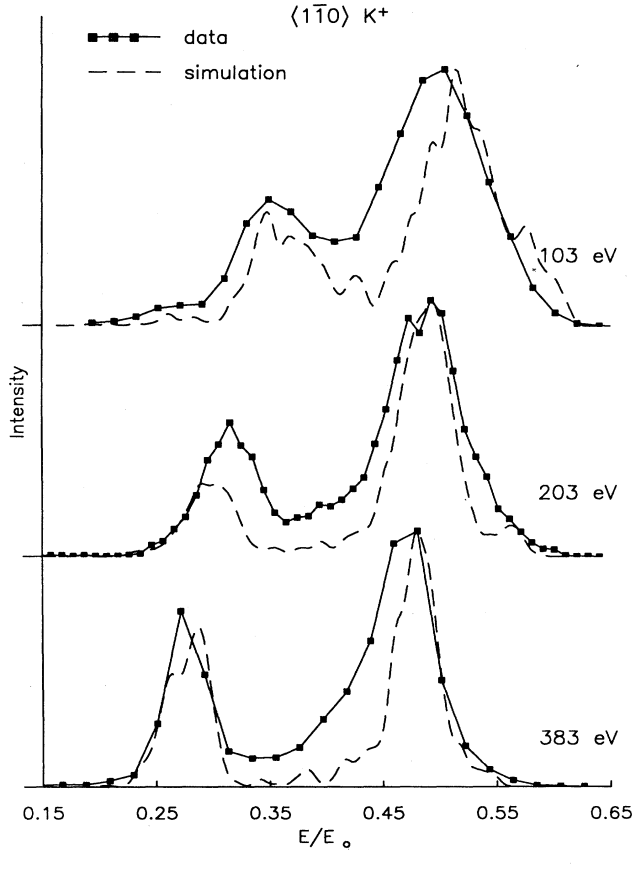

FIG. 10. Comparison of measured and calculated spectra for 90° specular scattering of K^+ along the ⟨1$\bar{1}$0⟩ azimuth of Cu(110) at incident energies of 103, 203, and 383 eV. The calculation was performed with the Hartree-Fock K^+-Cu pair potential and $V_{min}=3$ eV.

ing peak for 200- and 400-eV incident energies almost as well as the Hartree-Fock potential, even though it does very poorly on the focused single scattering energy. This demonstrates the greater sensitivity of focused scattering to the interaction potential.

The $\langle 1\bar{1}0 \rangle$ K^+ calculated spectra (Fig. 10) using the Hartree-Fock K^+-Cu potential also accurately reproduce the corresponding experimental energy peak positions. The peak ratios in the calculated 100- and 400-eV spectra agree well with the data, but the single to double intensity ratio in the calculated 200 eV spectrum is off by nearly a factor of 2, and the calculated backgrounds are generally low. The first-layer single scattering peak, which is distinctly visible at 100 eV incident energy, is barely visible in the simulated spectrum. The potassium simulations, like the sodium simulations, consistently underestimate the first-layer contribution to the scattering and the overall backgrounds, which, as we stated earlier, probably indicates an underestimate of the surface-atom vibration amplitudes.

The separation of the total ion-surface interaction into a sum of repulsive ion-atom pair potentials and a small attractive ion-conduction electron interaction $[V(z)]$ works well for the ion energies and scattering geometries described here. No enhancement of the repulsive part of the ion-surface potential with respect to a sum of ion-atom pair potentials was seen in these scattering experiments, nor was it evident in the other scattering geometries we have investigated.[14] This is consistent with the results of Horn *et al.*,[6] who found no many-body enhancement of the repulsive ion-surface interaction for 10–100-eV Na^+ and K^+ scattered from Ag(111). Their work with K^+ and Na^+ on W(110) below 50 eV,[8] however, found certain features of the K^+ scattering to be consistent with a breakdown of the sum of pair-potentials approximation. The observation of this many-body enhancement in this ion energy range (above 10 eV) apparently requires both a small ion-to-surface-atom mass ratio (to ensure a close approach of the ion to a surface atom) and a large electronic overlap between the ion and the surface atoms for ion-atom separations comparable to half the nearest-neighbor distance on the surface (to ensure a large overlap between the ion and at least two surface atoms simultaneously). Both of these conditions are adequately satisfied for K^+ on tungsten.[6] However, the mass ratio for K^+ on copper and silver is much larger than on tungsten, and even on W(110) no enhancement of the ion-surface repulsion was seen for Na^+ scattering (since the overlap is smaller), so it is not expected to be important for sodium scattering from copper or silver, which have smaller atomic numbers than tungsten.

CONCLUSIONS

We have shown that the interaction of 100–400-eV Na^+ and K^+ with Cu(110) can be very well described by a total ion-surface interaction which is the sum of Hartree-Fock pair potentials and an attractive imagelike potential. The sensitivity of the scattering to the interaction potential is enhanced by the strong focusing that occurs at these energies on Cu(110). The Hartree-Fock potentials are able to reproduce the variation of the focused single scattering peak energy as a function of incident energy, which the ZBL potential cannot do. The quality of the agreement between simulation and experiment shown here makes us confident that we can determine *in detail* the trajectories of scattered ions at these energies.[17] As the programs for calculating *ab initio* pair potentials become more available, we expect Hartree-Fock potentials will become the standard for interpreting ion scattering data over a wide range of incident energies.

ACKNOWLEDGMENTS

The authors wish to acknowledge fruitful discussions with E. Goldfield, K. Jacobsen, J. Sethna, M. Teter, and C. Umrigar. This work was supported by the U.S. Air Force Office of Scientific Research (Grant No. AFOSR-88-0069) and by the National Science Foundation (Grant No. NSF-DMR-84-51979). The simulations were done at the Cornell University Materials Science Center computing facility, which is supported in part by the National Science Foundation, and the Cornell Production Supercomputer Facility of the Center for Theory and Simulation in Science and Engineering, which is supported, in part, by the National Science Foundation, New York State, and IBM corporation.

[1] O. B. Firsov, Zh. Eksp. Teor. Fiz. **33**, 696 (1957) [Sov. Phys.—JETP **6**, 534 (1958)].
[2] R. K. Gordon and Y. S. Kim, J. Chem. Phys. **56**, 3122 (1972).
[3] J. J. C. Geerlings, L. F. Tz Kwakman, and J. Los, Surf. Sci. **184**, 305 (1987).
[4] G. A. Kimmel, D. M. Goodstein, and B. H. Cooper, J. Vac. Sci. Technol. A (to be published).
[5] P. J. van den Hoek, A. D. Tenner, A. W. Kleyn, and E. J. Baerends, Phys. Rev. B **34**, 5030 (1986).
[6] T. C. M. Horn, Pan Haochang, P. J. van den Hoek, and A. W. Kleyn, Surf. Sci. **201**, 573 (1988).
[7] E. Hulpke and K. Mann, Surf. Sci. **133**, 171 (1983).
[8] A. D. Tenner, K. T. Gillen, T. C. M. Horn, J. Los, and A. W. Kleyn, Phys. Rev. Lett. **52**, 2183 (1984).
[9] R. H. Ritchie, Phys. Rev. **114**, 644 (1959).
[10] M. T. Robinson and I. M. Torrens, Phys. Rev. B **9**, 5008 (1974).
[11] A. J. Algra, E. v. Leonen, E. P. Th. M. Suurmeijer, and A. L. Boers, Radiat. Eff. **60**, 173 (1982).
[12] A. J. Algra *et al.*, Radiat. Eff. **62**, 7 (1982).
[13] A. L. Boers, Surf. Sci. **63**, 475 (1977).
[14] D. L. Adler, D. M. Goodstein, and B. H. Cooper (unpublished).
[15] R. L. McEachern *et al.*, Rev. Sci. Instrum. **59**, 2560 (1988).
[16] D. M. Goodstein, S. A. Langer, and B. H. Cooper, J. Vac. Sci. Technol. A **6**, 703 (1988).
[17] R. L. McEachern, D. M. Goodstein, and B. H. Cooper, Phys. Rev. B **39**, 10 503 (1989).

[18]U. Gerlach-Meyer, E. Hulpke, and H. D. Meyer, Chem. Phys. **36**, 329 (1970).
[19]M. Copel, T. Gustafsson, W. R. Graham, and S. M. Yasilove, Phys. Rev. B **33**, 8110 (1986).
[20]M. J. Frisch *et al.*, GAUSSIAN86 (Carnegie-Mellon Quantum Chemistry Publishing Unit, Pittsburgh, 1984).
[21]I. Hyla-Kryspin, J. Demuynck, A. Strich, and M. Benard, J. Chem. Phys. **75**, 3954 (1981).
[22]*Gaussian Basis Sets for Molecular Calculations,* edited by S. Huzinaga (Elsevier, Amsterdam, 1984).
[23]*Handbook of Gaussian Basis Sets,* edited by R. Poirier, R. Kari, and I. G. Csizmadia (Elsevier, Amsterdam, 1985).
[24]M. J. Puska and R. M. Nieminen, Phys. Rev. B **27**, 6121 (1983).
[25]O. B. Firsov, Zh. Eksp. Teor. Fiz. **36**, 1517 (1959) [Sov. Phys.—JETP **36**, 1076 (1959)].
[26]J. P. Biersack and J. F. Ziegler, in *Ion Implantation Techniques,* Vol. 10 of *Springer Series in Electrophysics,* edited by H. Ryssel and H. Glawischnig (Springer-Verlag, Berlin, 1982).
[27]S. H. Overbury and D. R. Huntley, Phys. Rev. B **32**, 6278 (1985).